

# MultiPath Transfer Engine: Breaking GPU and Host-Memory Bandwidth Bottlenecks in LLM Services

Lingfeng Tang<sup>†1</sup> Daoping Zhang<sup>†1</sup> Junjie Chen<sup>1</sup> Peihao Huang<sup>\*1</sup> Feng Jin<sup>2</sup> Chengguang Xu<sup>2</sup> Yuxin Chen<sup>2</sup> Feiqiang Sun<sup>2</sup> Guo Chen<sup>\*1</sup>

<sup>1</sup>Hunan University  
<sup>2</sup>Tencent

## Abstract

The limited bandwidth of PCIe has emerged as the critical bottleneck for large language model (LLM) performance, such as prefix cache fetching and model switching. Although intra-server multipath data transfer between GPU and host memory is theoretically possible, heterogeneous protocols such as PCIe and NVLink currently limit the bandwidth between host memory and GPUs to that of a single PCIe link. This limitation results in underutilized intra-server bandwidth. To address this issue, we propose Multipath Memory Access (MMA), a scheme that, to the best of our knowledge, is the first to enable efficient multipath data transfer between GPU and host memory. MMA supports seamless deployment via dynamic library injection, enabling LLM applications to benefit from MMA without requiring any code modification. In our test-bed, MMA significantly improves the data transfer bandwidth between the GPU and memory, achieving a peak bandwidth of 245 GB/s—representing a 4.62× speedup compared to the native single-path bandwidth. End-to-end evaluations demonstrate that MMA reduces the time-to-first-token (TTFT) for LLM serving by 1.14× to 2.38× and decreases model-switching latency in vLLM’s sleep mode by 1.12× to 2.48×.

## 1 Introduction

High-throughput communication between the GPU and the host-memory is crucial. As the limited capacity of GPU memory is insufficient for large models, hindering their efficient execution [12, 33, 35]. Current machine learning (ML) systems have to offload inactive model weights [7, 33, 42] such as those used in vLLM’s Sleep Mode or prefix caches generated during the prefill phase to host-memory, and load them back to the GPU only when needed [14, 15, 21, 30, 50, 51].

The limited bandwidth of PCIe [31] has emerged as the critical bottleneck for LLM performance. As shown in §2.1,

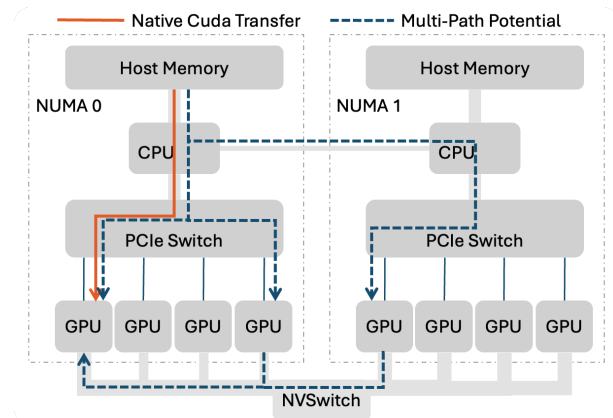


Figure 1: Simplified Intra-Server PCIe Topology. Each NUMA node contains two PCIe switches, and eight GPUs are interconnected via NVLink.

the read speed of the prefix cache directly impacts Time to First Token (TTFT), with prefix-cache retrieval alone accounting for up to 70% of TTFT. Likewise, in vLLM’s Sleep Mode, PCIe data transfer dominates the model-swapping path, contributing roughly 90% of the total switching latency.

Multipath transfer offers a promising way to break the PCIe bottleneck. Although PCIe remains the default route for moving model states between host-memory and GPUs, current ML systems, as shown in Figure 1, send nearly all host-to-GPU traffic through a single PCIe link (the red line). As shown in Table 1, the limited bandwidth of this path becomes the dominant constraint on end-to-end transfer performance. But modern servers always contain several additional intra-node\* parallel paths—NVLink, NVSwitch [27], and alternative NUMA [17] routes (the green dotted lines), which have more than ten times the bandwidth of PCIe but remain unused during host-memory to GPU transfers. Exploiting these idle paths alongside the directly attached PCIe link provides a natural opportunity for multipath transfer that can significantly widen the effective data bandwidth.

<sup>†</sup>Equal contribution (co-first authors)

\*Corresponding author

\*In this paper, we use intra-server, intra-node and intra-host interchangeably, which refers to the area inside a server machine.

Table 1: Bandwidth Comparison

Component Type	Specifications	Theoretical Bandwidth	Real-World Bandwidth
PCIe	PCIe 5.0 x16 [31] (unidirectional)	64 GB/s	52-60 GB/s
host-memory	Dual AMD EPYC 9005 [3] (DDR5-4800, 24 channels)	922 GB/s	600-700 GB/s
GPU memory	NVIDIA H20 96GB HBM3 [9]	4.0 TB/s	3.6 - 3.8 TB/s
NVlink	NVLink 4.0 [28]	900 GB/s	800-900 GB/s
CPU Interconnect	AMD EPYC 9654 Infinity Fabric [2](4 links)	1024 GB/s	600–750 GB/s

However, achieving efficient multipath intra-host transfer between GPU and host-memory still remains unsolved, which faces three key challenges that must be addressed. First, how to initiate multipath in a effective manner is itself highly challenging. The CPU lacks the authority to dynamically modify intra-server traffic, once a task is dispatched into the transfer pipeline, it effectively loses the ability to adjust its path, preventing fine-grained and dynamically changing multipath transfers. Moreover, due to restrictions at both the GPU hardware protocol layer and the driver layer, implementing multipath on the GPU side without modifying GPU hardware is nearly impossible—and altering GPU hardware is prohibitively complex. Moreover, introducing multipath transfer through middleware makes preserving dependency correctness on the GPU a new problem. GPU tasks must strictly follow dependency constraints, but middleware-based multipathing obscures the original dependency visibility, making it difficult for the GPU to enforce them correctly.

Second, without accurate link-state visibility, it is difficult to precisely allocate data across paths so that bandwidth is fully utilized without causing overflow. Unlike datacenter network protocols that benefit from rich mechanisms for probing network state, intra-host communication lacks visibility into link-level conditions. The runtime therefore operates in a near-blind setting, where static or heuristic traffic splitting quickly leads to persistent underutilization. Requiring new designs that can make reasonable load-balancing decisions under a largely stateless environment.

Finally, integrating such mechanisms into existing ML frameworks while ensuring transparent usage and minimizing additional latency poses substantial engineering challenges. At the hardware-protocol level, current servers offer no native support: each GPU’s PCIe link is statically tied to a specific NUMA node, and a GPU’s PCIe controller can only reach the CPU memory controller directly attached to it. This prevents a GPU from borrowing another GPU’s PCIe path for data movement. Worse still, the software stack provides little help either. Although host physical memory is globally addressable, existing drivers require every DMA operation to obey three static constraints: issuing privilege, IOMMU [20] mapping, and physical routing—and expose no mechanism for a GPU to proxy another GPU’s DMA or share PCIe channels. As a result, enabling transparent intra-host cross-GPU relay

requires building a nontrivial mediation layer atop these rigid constraints.

This paper presents MMA, the first intra-server *Multipath Memory Access* transport between GPU and host-memory that addresses all aforementioned challenges. Specifically, MMA introduces a novel dummy task that retrieves control from asynchronous transfer tasks, along with a synchronization mechanism to maintain the original dependencies. This design enables the CPU to dynamically schedule multipath transfers according to real-time path congestion. Second, we design a congestion-aware routing strategy that achieves intra-server traffic load balancing even in the absence of path-aware information. Finally, MMA provides a fallback mechanism to maintain the original transfer efficiency of small data, and a dual-pipeline relay mechanism to improve GPU relay efficiency.

We have implemented MMA prototype in CUDA 12.8 [26] with 3000 line C++ codes [1]. We evaluated MMA on a standard NVIDIA H20 GPU platform with PCIe 5.0 ×16 and NVLink 4.0. Results shows that MMA significantly improves the data transfer bandwidth between the GPU and memory, achieving a peak bandwidth of 245 GB/s—representing a 4.62× speedup compared to the native single-path bandwidth. End-to-end evaluations demonstrate that MMA effectively accelerates ML tasks plagued by traffic imbalance: it reduces the TTFT of LLM serving by 1.14–2.38× and shortens the model switching time in vLLM’s Sleep Mode [47] by 1.12–2.48×.

In summary, we make the following contributions: 1) We present MMA, the first multipath memory access for intra-server GPU and Host-Memory. 2) We integrate MMA into CUDA, enabling ML applications to benefit from it seamlessly. 3) Testbed results shows MMA effectively improves intra-server GPU bandwidth and ML tasks efficiency under imbalanced traffic.

## 2 Background and Motivation

As LLMs with hundreds of billions of parameters advance, machine learning’s storage demands have far exceeded GPU memory capacity. In addition to performing large-scale parallel computations, GPUs must efficiently manage and transfer working sets that surpass their memory limits [4, 21, 24, 32]. To address this, modern systems offload parts of the model or

runtime state to host-memory, dynamically transferring them to the GPU as needed via host-to-device (H2D) and device-to-host (D2H) communication over PCIe. This approach helps alleviate memory pressure in GPU-accelerated LLM inference, ensuring continuous model execution even when the working set exceeds GPU memory capacity. However, PCIe bandwidth has become a new bottleneck for system performance.

## 2.1 The Necessity to Accelerate GPU-to-Host Memory transfer

We present several typical cases and some results measured in our H20 GPU testbed (detailed testbed settings in §5.1.2), to show how transfer between GPU-and host-memory limits the whole system’s performance.

**The time to fetch cache from host-memory accounts for up to 70% of the total TTFT.** Systems like vLLM [21] and HuggingFace Accelerate [16] offload long sequence key-value caches, which cannot fully fit into GPU memory during autoregressive decoding, to host-memory. This results in frequent D2H/H2D transfers as page caches are transferred between the host and GPU. The speed of fetching this cache has a direct and substantial impact on latency-critical metrics TTFT. We measure the TTFT for prefix cache hits under different context lengths using the LMCACHE+vLLM [11] inference framework with prefill–decode disaggregation. As shown in Figure 2, prefix cache fetching time can account for up to 70% of the total TTFT, when 64k token hits on the Qwen-7B-Chat [5] model. This proportion increases with the context length and is further affected by model hyper-parameters, including hidden size, number of hidden layers, attention heads, and KV heads. Moreover in real-world applications like multi-turn conversations, code generation, and retrieval-augmented generation, context lengths often exceed 100k tokens [19], further exacerbating the impact of prefix cache transfer latency.

**The time to load/store models from/to host-memory accounts for up to 90% of the model switching.** In vLLM’s Sleep Mode (Level 1), switching between different specialized models is permitted to improve GPU utilization. The mode first swaps out model weights from GPU memory to host-memory via D2H transfers(fall-asleep), then swaps in the weights of a newly loaded model from host-memory back to GPU memory via H2D transfers(wake-up). We evaluated the data transfer overhead of vLLM’s Sleep Mode [47]—i.e., model swap in and swap out by Level 1 sleep across models [5, 49] of different sizes. As shown in Figure 3, data transfer increasingly dominates total model swap latency as the model size grows—ranging from 40–50% for 0.6B parameters, about 75% for 4B parameters, and exceeding 85–95% for the 32B parameters.

## 2.2 Need for multipath memory access

Although a single PCIe lane becomes the bottleneck, enabling multipath intra-host transfers is fundamentally feasible at the physical layer. In contemporary GPU servers, multiple GPUs coexist, each connected to host-memory via PCIe while also forming a Tbps-scale, fully connected fabric through NVLink. This architecture provides an opportunity to exploit the idle PCIe and NVLink bandwidth of other GPUs to assist in multipath data transfers, thereby alleviating the pressure on the primary PCIe path.

Furthermore, we observe that the PCIe traffic generated by LLM applications is inherently imbalanced, and relay a portion of the traffic through other GPUs’ idle PCIe/NVLink bandwidth does not interfere with their normal communication. To quantify this effect, we monitored intra-server traffic utilization across different PCIe links while running LLM services with decoupled prefill and decoding stages using the public dataset [25]. As shown in Figure 4a, the load does not simultaneously consume all PCIe bandwidth, some PCIe links remain significantly underutilized, whereas others experience heavy load. We further analyzed the temporal dynamics of model switching using the Chatbot Arena dataset [29] on an 8-GPU server and correlated it with the corresponding PCIe traffic. As shown in Figure 4b, the switching behavior induces highly skewed and bursty PCIe load patterns, reinforcing the opportunity to exploit unused bandwidth on neighboring GPUs.

## 2.3 Multipath memory access challenges

Leveraging the high-speed interconnect capabilities between GPUs, multipath transfer schemes can optimize data transfer between the GPU and host-memory, thereby improving overall link utilization. However, to realize efficient intra-server Multipath Memory Access transport, MMA needs to address the following key challenges.

**How to dynamically transfer tasks after they have been statically assigned by CPU?** Once the CPU statically enqueues tasks to a sending queue, the transfer paths are fixed and cannot adapt to dynamic intra-node traffic. Allowing the CPU to dispatch tasks dynamically would increase complexity on the user side and require frequent synchronization points, causing CPU–GPU stalls and reducing overall efficiency.

MMA intuition. We observed that introducing an intermediate layer to intercept tasks, without modifying underlying hardware or user programs, provides an effective way to enable multipath transfer. However, reducing latency while maintaining transparency remains a challenge. To this end, MMA implements a Transfer Task Interceptor that filters small transfers through a scheduler to ensure low latency, while buffering large transfers in the multipath sending engine until they receive dispatch permission. Carefully designed dummy tasks maintain the original task dependencies, ensur-

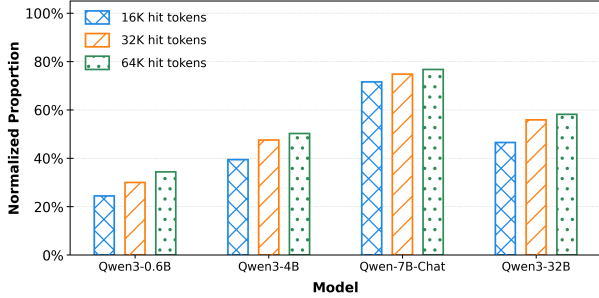


Figure 2: The proportion of prefix-cache fetching time in TTFT under different hit-token lengths and models

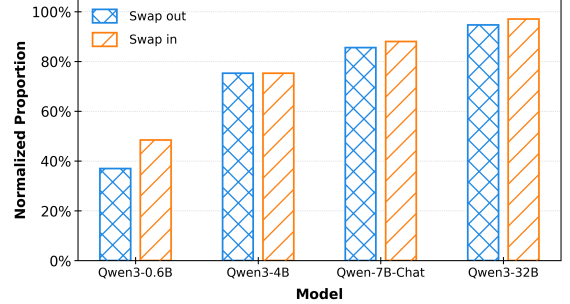
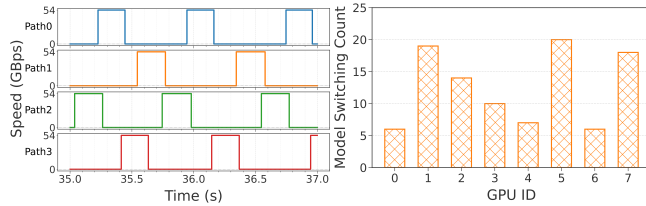


Figure 3: The proportion of H2D/D2H transfer time in swap-in and swap-out latency under different models



(a) Prefix cache fetching (b) Model switching  
Figure 4: Traffic imbalance in LLM applications

ing correct execution. As such, MMA achieves efficient multipath transfers transparently, without requiring any changes on the user side or exposing the underlying complexity.

**How to ensure GPU tasks follow dependency constraints during multipathing?** CPU-issued transfer tasks must be executed in a dependency order. Subsequent tasks establish dependencies with the preceding tasks in the transfer queue. When the GPU receives a task, it receives the dependencies and transfers accordingly. However, if the intermediate layer intercepts and inserts dummy tasks, the GPU cannot perceive the dependencies or completion status of the real tasks through them, leading to system errors. Without modifying the hardware or drivers, a clever design of the intermediate layer and existing tools is needed to achieve fast and accurate synchronization between the dummy tasks and the real tasks.

**MMA intuition.** We discovered that while dummy tasks cannot execute transport tasks, but they can carry synchronization information back and forth between the CPU and GPU. Therefore, we designed a synchronization module that analyzes dummy task information fed back from other modules to control the start and end of transport tasks, achieving synchronization between dummy tasks and transport tasks and maintaining the correct execution of dependencies.

**How to precisely allocate data across paths without accurate link-state visibility?** Unlike data center networks, where ACKs carry ECN, RTT, and other information to reflect link congestion, PCIe does not expose explicit congestion signals to upper layers. Existing load balancing and congestion control mechanisms do not consider this situation; Random packet distribution may exacerbate congestion on a particular

path, leading to unpredictable jitter and long-tail latency.

**MMA intuition.** We observe that accurate load balancing is possible even without explicit congestion signals. By allocating a dedicated sending buffer for each destination, the remaining tasks in the buffer provide an effective proxy for link congestion. In this insight, MMA introduces a two-level sending buffer mechanism. The second-level buffer reflects the current congestion on each destination PCIe link, while the first-level buffer enables flexible scheduling of transfer tasks. This design allows MMA to dynamically balance load across multiple paths without requiring hardware-level congestion feedback.

### 3 MMA Design

#### 3.1 Overview

MMA exploits the connection topology within servers—both between the Host and GPU accelerators and among multiple GPUs—to enable GPUs to act as relay nodes. This design transforms Host-GPU memory transfers from static single-path routing to dynamic multipath transfer, achieving load balancing across heterogeneous links. The primary design objective of MMA is to realize efficient multipath transfers while preserving the semantics of existing transfer APIs.

As shown in Figure 5, three core components of the MMA framework comprise: **Transfer Task Interceptor** §3.2. Responsible for replacing native transfer tasks with Dummy Tasks and submitting them to the GPU Runtime, while concurrently submitting the original transfer tasks to the multipath Transfer Engine for execution. **Sync Engine** §3.3. Ensures synchronization between the execution lifecycles of transfer tasks and Dummy Tasks, thereby maintaining consistent task coordination. **Multipath Transfer Engine** §3.4. Executes multipath transfer tasks, supporting concurrent management and scheduling of multiple transfer streams.

To get a high-level view of how the whole system works, here is a brief work flow of MMA.

The interceptor captures the native GPU transfer tasks and replaces them with Dummy Tasks which are submitted to the GPU runtime task queue. Meanwhile, the actual transfer

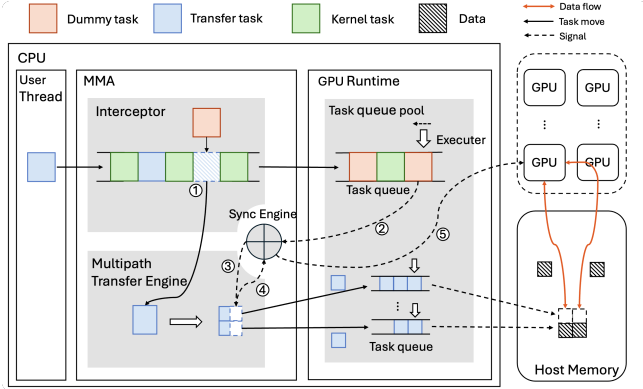


Figure 5: Overview of MMA.

tasks are relayed to Multipath Transfer Engine(①). When the GPU executes a Dummy Task, it notifies the Sync Engine(②). Upon receiving the notification, the Sync Engine instructs the Multipath Transfer Engine to start the multipath transfers(③). After the multipath transfer tasks are complete, the Multipath Transfer Engine sends a completion signal back to the Sync Engine(④). The Sync Engine then informs the GPU that the corresponding Dummy Task has been completed, triggering the execution of subsequent tasks(⑤).

### 3.2 Transfer Task Interceptor

To enhance the cooperative efficiency between the CPU and GPU, an asynchronous operation mode is commonly employed in contemporary systems. Specifically, after the CPU dispatches tasks, the GPU asynchronously receives and executes subsequent computations, thereby mitigating idle GPU time that would otherwise result from waiting for CPU task submissions.

However, this asynchronous paradigm introduces challenges for multipath data transfers between the CPU and GPU. When the CPU issues multiple transfer tasks, the GPU does not immediately perform these multipath transfers, as it may still be executing earlier asynchronous tasks submitted by the CPU. Consequently, by the time the GPU executes the multipath transfers, the internal congestion state of the system may have altered, negatively impacting the overall efficiency of multipath transfers.

A potential solution is to endow the GPU itself with multipath transfer capabilities. Upon receiving transfer tasks, the GPU could adaptively perform multipath transfers based on the current host network traffic and topology. Nevertheless, such a solution necessitates hardware-level support from the GPU, which is currently absent in commercially available GPU architectures.

MMA provides an elegant solution that improves multipath transfer efficiency without modifying GPU hardware and while preserving the original asynchronous programming

model. MMA introduces a Transfer Task Interceptor, which intercepts user-submitted transfer tasks and substitutes them with Dummy Tasks—i.e., placeholder tasks dispatched to the GPU. Instead of being directly dispatched to the GPU asynchronously, the original transfer tasks are blocked in the task queue of the multipath transfer engine. The blockage is released only when the Dummy Task begins execution. At this stage, the multipath transfer engine dynamically schedules transfers in accordance with the current traffic conditions, initiating multipath transfers accordingly.

Given that MMA’s multipath data transfer incurs additional overhead and may increase latency for small transfer tasks, the Transfer Task Interceptor incorporates a Fallback Mechanism. To mitigate the additional overhead and increased latency incurred by MMA’s multipath data transfer during small transfer tasks, MMA introduced a Fallback Mechanism within the Transfer Task Interceptor.

Transfer tasks with data sizes below a specific threshold automatically revert to native single-path transfer bypass Multipath Transfer Engine. The fallback threshold is related to the multipath data chunk size. The chunk size configuration should reference the Task Manager design (§ 3.4.1), and the optimal fallback threshold can also be empirically determined through experimentation in §5.1.3.

### 3.3 Sync Engine

Since MMA replaced the original Transfer Task with a Dummy Task, all tasks that previously depended on the Transfer Task now depend on the Dummy Task. To ensure the correctness of inter-task dependencies, the execution lifecycles of Dummy Tasks and their corresponding transfer tasks must be synchronized.

One feasible implementation is to embed the transfer task metadata within the Dummy Task, so that when the GPU executes the Dummy Task, it notifies the Multipath Transfer Engine to initiate the corresponding transfer and monitors the transfer task’s status to determine completion. However, this approach currently requires modifications to GPU hardware and drivers, which are not supported.

MMA designed a Sync Engine that leverages existing GPU runtime callback interfaces (e.g., NVIDIA CUDA’s `cudaStreamAddCallback` API) without extensive hardware modifications. When the GPU reaches the Dummy Task, a callback is triggered to notify the Sync Engine to start the associated transfer task. Simultaneously, a spin kernel is launched on the GPU to prevent premature termination of the Dummy Task and thereby maintain its execution lifecycle. Finally, by utilizing the GPU’s Unified Memory mechanism, the Sync Engine receives a notification upon transfer task completion and subsequently releases the spin kernel, thereby achieving synchronized execution between the Dummy Task and the transfer task. The detailed implementation of spin kernel is described in §4.

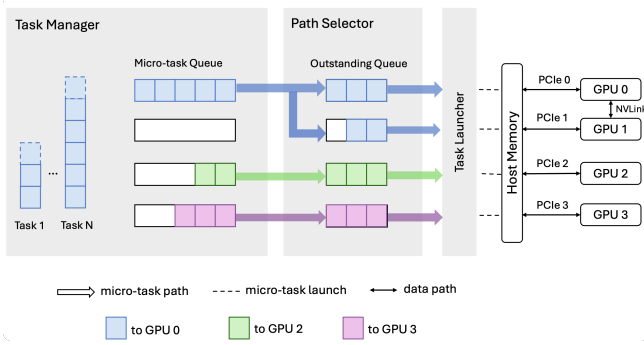


Figure 6: Transfer Engine. Different color refers to different destination of micro-tasks.

### 3.4 Multipath Transfer Engine

This section will introduce the design of the Multipath Transfer Engine. As illustrated in Figure 6, the Multipath Transfer Engine consists of three core components: the Task Manager, which manages the lifecycle of Tasks and the size of data segmentation; the Path Selector, which performs path selection based on load balancing; and the Task Launcher, which issues concrete transfer Tasks according to the selected paths. This design enables efficient scheduling and execution of transfer operations.

#### 3.4.1 Task Manager

To enable multipath transfer, upon receiving the synchronization signal from the Sync Engine indicating the start of the Dummy Task execution, the Task Manager divides the original transfer task into multiple micro-tasks according to a fixed chunk size. Each micro-task corresponds to a batch of data, which is then sequentially submitted to the Micro-task Queue for transfer.

After all micro-tasks have been successfully transferred, the Task Manager notifies the Sync Engine that the transfer task is complete and subsequently terminates the associated Dummy Task, thereby ensuring synchronized management of task execution states.

With regard to data chunking, the Task Manager configures the granularity of data chunks to effectively control load imbalance across links within an acceptable range, thereby promoting efficient multipath transfer. The choice of chunk size involves a trade-off: overly small chunks fail to fully utilize bandwidth, while excessively large chunks reduce the granularity of load balancing. Further details are provided in §5.1.3. Consequently, the transfer engine dynamically adjusts the chunk size based on system architecture and runtime environment to achieve balanced load distribution.

Once the original transfer task is partitioned into micro-tasks with appropriate chunk sizes, effective management of these micro-tasks becomes essential to realize efficient multipath transfer. To address this, the MMA design introduces

a Micro-task Queue mechanism to organize and schedule micro-tasks efficiently. As illustrated in Figure 6, the Task Manager arranges transfer tasks into queues indexed by their target GPU, grouping all tasks destined for the same GPU into a single queue. This design enables the Path Selector to prioritize direct-path scheduling strategies, thereby improving transfer efficiency.

Additionally, Micro-task Queues can be managed using priority queue mechanisms inspired by computer networks, overcoming the limitation that memory-to-GPU communication does not natively support priority scheduling. Overall, the Task Manager enables more diverse and flexible options for intra-server traffic scheduling.

#### 3.4.2 Path Selector

As mentioned in §2.3, the asymmetric communication semantics between the CPU and GPU make it difficult to implement feedback mechanisms in PCIe environments. Additionally, congestion monitoring introduces significant overhead and demands careful tuning to avoid scheduling delays. These inherent challenges complicate effective multipath load balancing in PCIe systems.

To address these issues, MMA employs a congestion-aware routing strategy in Path Selector, leveraging the native flow control features of PCIe and NVLink protocols. Rather than relying on active probing, it passively infers congestion from the depth of Outstanding queues, enabling efficient routing decisions without incurring additional signaling overhead.

Specifically, MMA maintains an outstanding queue for each PCIe link, with each queue statically bound to a specific GPU based on the PCIe topology. The task launcher retrieves micro-tasks from these queues and dispatches them onto their corresponding PCIe links. For example, in H2D tasks, if the micro-task’s destination GPU matches the outstanding queue’s assigned GPU, it travels over a direct PCIe link. Otherwise, it takes a relay path involving the PCIe link plus an NVLink connection between GPUs.

Due to the inherent flow control mechanisms of PCIe and NVLink, congestion on a link will block the head micro-task in the outstanding queue, preventing it from fetching new tasks from the micro-task queue. Conversely, links without congestion can continuously consume micro-tasks, effectively redistributing workload from congested links and thus achieving load balancing.

Based on this strategy, MMA have further carried out the following optimizations and discussions.

**Direct path first.** For relay path, NVLink is employed to route data fragments to the target GPU, incurring additional bandwidth consumption. To mitigate this overhead, MMA adopts a direct path first strategy, ensuring that the Outstanding queue corresponding to each GPU always has priority in fetching transfer tasks from the associated Micro-task Queue, as shown in Figure 6. This direct path first approach avoids introducing

GPU peer-to-peer (P2P) communication, maximizing utilization of the intra-server network bandwidth, detailed in §5.1.3.

**Relay task scheduling.** Since we use a direct path first strategy, the outstanding queue prioritizes completing direct tasks before processing micro-tasks from other queues, which can be considered relay tasks. In this context, several scheduling approaches can be applied: by prioritizing tasks from the longest micro-task queue, the system ensures that the overall number of direct tasks is maximized, thereby reducing the additional bandwidth consumption on NVLink. Alternatively, if the goal is to prioritize data transfer for a specific GPU—either as a source or destination—tasks can be preferentially fetched from the corresponding micro-task queue.

**Contention with background traffic.** When a flow on a particular link experiences contention with background traffic, its outstanding queue can become blocked. To address this, two different strategies can be employed: if prioritizing background traffic is desired, the outstanding queue can wait for a period after being blocked before fetching micro-tasks from the micro-task queue; alternatively, if the goal is to prioritize the transfer of the task or to maximize link utilization, the outstanding queue can immediately retrieve micro-tasks as soon as there is available space, minimizing idle time and making more efficient use of the link.

### 3.4.3 Task Launcher

The Task Launcher is responsible for dispatching specific transfer tasks to the GPU via the GPU Runtime interface, where the GPU executes the actual data plane transfer. Specifically, the Task Launcher issues different GPU operations depending on the type of micro-task. Taking H2D tasks as an example, for direct tasks, a single H2D transfer operation is issued, and the GPU’s internal DMA engine handles the data transfer. Conversely, for relay paths, both an H2D operation and a P2P operation between GPUs must be issued, with a dependency established between these operations to guarantee the correctness and ordering of data transfer.

To enhance relay efficiency on the GPU, MMA adopt a dual-pipeline relay mechanism as illustrated in Figure 7(b). This approach effectively avoids the transfer bubbles observed in PCIe and NVLink links under a single-pipeline relay scheme shown in Figure 7(a). The proposed dual-pipeline design significantly improves bandwidth utilization during relay and enhances overall system performance.

**GPU Relay Overhead.** In the practical deployment, we utilize the ordering property of CUDA streams to implement a pipelined relay mechanism for H2D P2P communications. Both H2D and P2P transfers utilize the GPU’s dedicated DMA engine, which handles data movement independently without occupying the GPU’s compute resources such as the Streaming Multiprocessors (SMs), registers, shared memory, or thread schedulers. To support dual-pipeline relay, we add two relay streams on each GPU. Each relay stream has a ded-

icated relay buffer to store the data chunks to be forwarded. The memory overhead of each relay buffer is limited to one data chunk. In our deployment, the chunk size is set to 5 MB, detailed in §5.1.3. Thus, the total GPU memory overhead is calculated as

$$2 \times 2 \times 5 \text{ MB} = 20 \text{ MB},$$

accounting for bidirectional traffic and dual pipelines. This memory overhead is acceptable for modern GPUs.

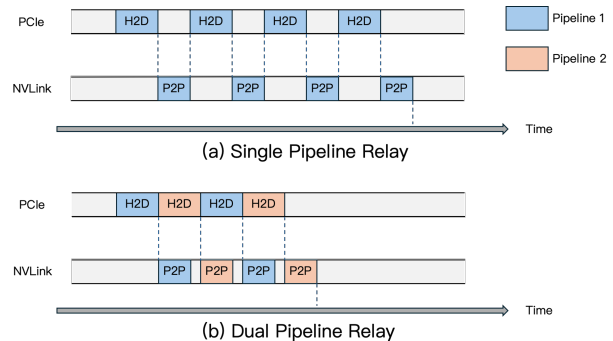


Figure 7: Task Launcher use dual pipeline relay mechanism to optimize the utilization of PCIe and NVlink.

## 4 Implementation

MMA is built on the NVIDIA platform using CUDA 12.8. The deployment of the MMA system is completed with over 3000 lines of C++ code. Users can load the MMA dynamic library via the LD\_PRELOAD mechanism, achieving transparent substitution for the native CUDA memory API, facilitating integration and use.

This section details the key technical implementations of MMA, covering two technicals: Multipath Transfer Engine, and the Spin Kernel.

**Multipath transfer Engine.** To implement a passive routing mechanism based on the Outstanding queue, MMA allocate two threads per GPU (corresponding to each Outstanding queue): a transfer thread and a synchronization thread.

The transfer thread continuously monitors the Outstanding queue using busy-waiting. When the queue is not full, it promptly fetches new transfer tasks from the Mico-task Queue. After launching the task to the GPU via the Task Launcher, the transfer thread records a synchronization point by creating a CUDA event and then submits the corresponding synchronization task to the synchronization thread.

The synchronization thread handles synchronization tasks by calling cudaEventSynchronize, blocking until the transfer task completes. Once finished, it removes the task from the Outstanding queue and checks whether all the fragments of this transfer task have been fully transferred.

If all fragments have completed transfer, the synchronization thread notifies the Dummy Task on the GPU through the Sync Engine, indicating that the transfer task has ended.

**Spin Kernel** To achieve execution synchronization between the Dummy Task and the Transfer Task, MMA designed a spin kernel. Specifically: 1) A control flag variable `h_flag` is set in host CPU memory and bound via CUDA Unified Memory or zero-copy technology to a device variable `d_flag` in GPU memory, enabling implicit synchronization of modifications without explicit data transfer by sharing memory between host and device. 2) When the GPU kernel executes to the Dummy Task, it enters the following spin loop. It continuously monitors the device variable status. 3) When the Multipath Transfer Engine completes multiplexing, it sets `h_flag` to 1. Through the memory mapping mechanism, this update is immediately observed by the device, causing the kernel to exit the spin loop, finish waiting, and resume execution.

## 5 Evaluation

In this section, we first evaluate MMA’s overall performance. Then, we evaluate properties of MMA algorithm using a series of targeted experiments.

**Evaluation testbed** All experiments run servers with AMD EPYC 9654 Infinity Fabric CPU, eight NVIDIA H20 GPUs. The GPUs are connected via 18-lane NVLink and NVSwitch, delivering up to 478 GB/s one-way bandwidth for intra-server GPU–GPU communication, and each GPU is attached to the CPU complex through PCIe 5.0. We deploy MMA as a user-space shared library that intercepts CUDA H2D/D2H calls and routes transfer chunks over multiple PCIe paths using NVLink relays when needed.

**Methods compared** We use native CUDA memory copy as the baseline when performing intra-server GPU communication. In the baseline experiment, the traffic is statically bound to one PCIe for CPU-GPU communication

### 5.1 Microbenchmarks

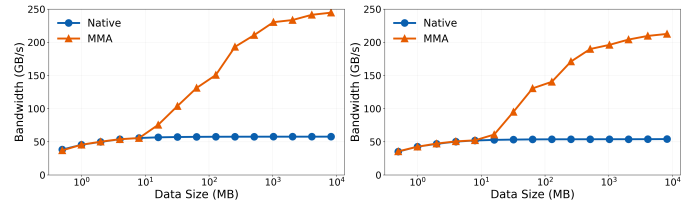
#### 5.1.1 Bandwidth improvement

We evaluate MMA’s bandwidth improvements over the baseline for host-to-GPU transfers across various message sizes.

**Setup** We test the message size from 1 KB up to 8 GB and compute the effective bandwidth as message size divided by completion time, averaging over multiple runs.

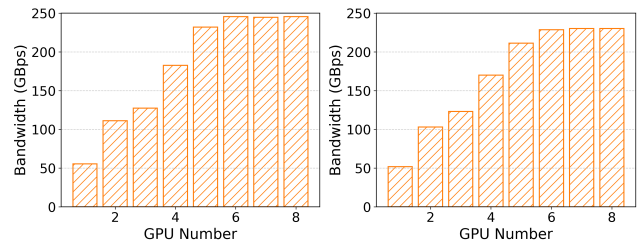
As shown in Figure 8, MMA’s data transfer performance surpasses the baseline starting at approximately 10MB of data size and approaches its theoretical bandwidth limit of 245GB/s around 1GB. In contrast, the baseline’s bandwidth bottleneck is approximately 53GB/s, resulting in a performance improvement of about  $4.62\times$  speedup. In LLM applications, the size of the intra-node H2D and D2H transfer tasks, such as KV cache and model parameters, typically ranges from several hundred megabytes to tens of gigabytes, thereby fully utilizing the high transfer capacity of MMA.

Furthermore, as shown in Figure 9, transfer bandwidth saturates when the number of participating GPUs reaches six. This saturation occurs because typically four GPUs reside within a single NUMA node, while cross-NUMA H2D transfers rely on the UPI link for data communication. As the number of cross-NUMA GPU relay tasks increases, the UPI link bandwidth becomes the limiting factor in overall system transfer performance.



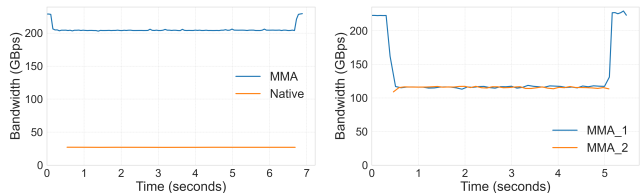
(a) H2D transfer bandwidth (b) D2H transfer bandwidth

Figure 8: Bandwidth performance with transfer task size for H2D and D2H transfers.



(a) H2D transfer bandwidth (b) D2H transfer bandwidth

Figure 9: MMA transfer bandwidth versus number of paths.



(a) MMA congestion with Native (b) MMA congestion with MMA CUDA

Figure 10: Bandwidth variations during congestion events under MMA and Native transfer methods.

#### 5.1.2 Robustness and Load Balancing

We evaluate how robust MMA is under contention and how well it balances load across paths. Our *baseline* configuration is that both streams use native `cudaMemcpyAsync` with static binding to fixed PCIe links as shown in Figure 1.

**MMA Coexistence with native CUDA traffic.** We first test how our MMA behaves when sharing PCIe with native `cudaMemcpyAsync` traffic. Here, native copies act as background traffic produced by “third-party” components (e.g., NIC DMA

or applications not using our library) and pin one direct PCIe link for a long period. Figure 10a illustrates the bandwidth allocation when native single-stream CUDA traffic coexists with MMA’s multi-stream transfer traffic. It can be observed that on congested links, MMA and native CUDA traffic achieve a fair bandwidth distribution, while on non-contended links, MMA’s bandwidth remains unaffected. This behavior arises because MMA strives to avoid bandwidth underutilization by ensuring continuous transfer tasks on each transfer path. Under the influence of internal PCIe flow control, a fair bandwidth sharing between MMA and native single-stream traffic is realized.

**MMA congestion with MMA.** Next, we examine interference between two concurrent MMA flows. As shown in Figure 10b, these two MMA flows fairly share the bandwidth, with the total bandwidth approaching the ideal value. This is because each process in MMA maintains its own multipath queue and pull-based scheduler; therefore, theoretically, the two flows might interfere with each other, but the bandwidth of both flows is still much higher than the native baseline.

**Load balancing: Dynamic MMA vs. static scheduling.** To evaluate the adaptability of MMA to dynamic traffic intra-node, we conducted a controlled experiment comparing the dynamic scheduling of MMA with static scheduling and native single-path transfer in scenarios with and without background traffic. For simplicity, the number of transfer paths was restricted to two and two static packet distribution ratios, 1:1 and 1:2, were analyzed.

As shown in Figure 11, the dynamic scheduling of MMA consistently achieves near-optimal load balancing in both scenarios, while static packet distributions only perform well under specific traffic patterns. This indicates a fundamental incompatibility between traditional GPU static graph execution and dynamic intra-node traffic conditions. MMA effectively addresses this challenge, enabling more stable and efficient data transfer. In the absence of background traffic, the two paths have identical bandwidths, making the 1:1 packet split capable of achieving ideal load balancing. However, in background traffic, PCIe flow control within the node reduces the bandwidth of congested paths to approximately half that of uncongested ones. In this case, a 1:2 packet distribution better approximates optimal load balancing.

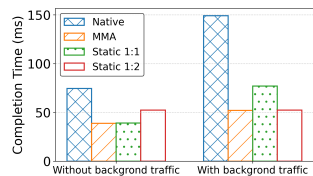


Figure 11: Compare of Completion time with and without background traffic.

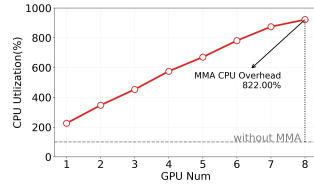


Figure 12: Comparison of CPU overhead with and without MMA.

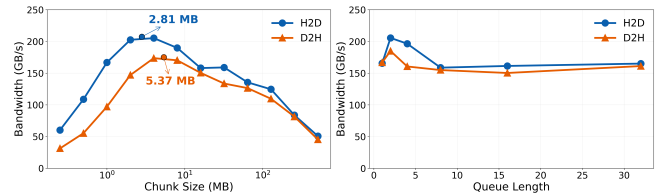
### 5.1.3 Deep Dive

#### Direct Priority prevents unnecessary NVLink traffic.

To measure whether Direct Priority can avoid unnecessary NVLink traffic, we simulated the simultaneous transfer of eight H2D tasks. As shown in Table 2, show that the GPU P2P bandwidth of MMA is essentially equivalent to the baseline scenario without any transfer tasks, effectively avoiding unnecessary NVLink traffic; disabling this strategy (MMA without direct priority) reduces P2P transfer performance by approximately 30GBps. This is because when Direct Priority is enabled, the GPU executing the direct transfer task will not actively accept forwarded tasks. Thereby avoiding wasting onboard PCIe bandwidth and prevents unnecessary NVLink traffic.

Table 2: Influence of Direct Priority on P2P Bandwidth

Method	GPU P2P Bandwidth (GBps)
P2P_alone	367.60
MMA	367.28
MMA without direct priority	330.56



(a) Chunk Size

(b) Queue Length

Figure 13: The relationship between Chunk size, Queue Length, and MMA Bandwidth.

#### Impact of Chunk Size and Outstanding Queue Length on MMA Bandwidth.

We experimentally measured the bandwidth performance of chunk size and incomplete queue length on MMA transfer bandwidth under a 512MB transfer task. As shown in Figure 13, H2D transfer achieves optimal bandwidth at a Chunk Size of approximately 2.81MB, while D2H transfer attains optimal bandwidth at around 5.37MB. Additionally, an Outstanding Queue Length of 2 results in peak bandwidth performance for both H2D and D2H paths. Small chunk sizes tend to degrade GPU data transfer efficiency due to overhead associated with processing numerous small tasks, whereas excessively large chunk sizes lead to coarse scheduling granularity that impairs load balancing. Similarly, an excessively long Outstanding Queue Length exacerbates the coarse granularity problem, further deteriorating load balancing. In contrast, setting the queue length to 1 causes idle waiting intervals after each transfer task completion while awaiting the next data chunk to queue. Given that the enqueue time for data chunks is generally shorter than the transfer task completion time, an Outstanding Queue Length of 2 allows

for the most efficient pipeline transfers.

**MMA optimal Fallback threshold.** The experiment evaluated the optimal Fallback threshold. In test environment, the MMA chunk size was configured to 5 MB. As shown in Figure 14, the corresponding break-even thresholds for H2D and D2H transfers were 11.3 MB and 13 MB, respectively, and the optimal threshold falls between two and five chunks, depending on the MMA-induced overhead and the effective internal transfer bandwidth.

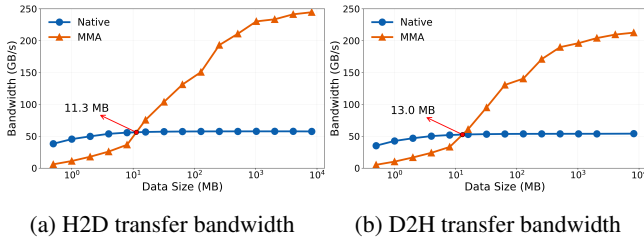


Figure 14: Optimal threshold of MMA fallback.

**MMA CPU Overhead.** The implementation of MMA relies on the CPU, resulting in additional CPU overhead. Figure 12 illustrates the relationship between CPU overhead caused by MMA and the number of GPUs, showing a linear increase in CPU overhead as the number of GPUs grows. When scaling up to 8 GPUs, the additional CPU overhead introduced by MMA peaks at 822%. This is primarily because MMA requires launching dedicated transfer and synchronization threads for each GPU. However, such overhead is acceptable in the context of LLM applications, where GPUs typically handle heavy computational loads while CPUs remain largely idle.

## 5.2 End-to-End Evaluation

In this section, we evaluate our system in two workloads of realistic LLM serving scenarios: (1) prefix cache prefill, where a long cached KV prefix must be transferred from host to GPU before decoding; (2) model switching under sleep/wake, where model weights need to be moved between CPU and GPU.

**Baseline.** Our baseline is the native CUDA implementation with static single-path binding between the CPU and the target GPU over one PCIe link. We report end-to-end improvements on TTFT and model switching latency.

### 5.2.1 Prefix cache prefill

**Setup.** We evaluate how MMA affects TTFT when prefix cache hits under the LMCache+vLLM [11] inference framework with prefill-decode disaggregation. We use four LLMs with different architectures (and therefore different KV-cache sizes at the same sequence length): Qwen2.5-7B-Instruct, Qwen3-4B, Qwen-7B-Chat, and Qwen3-32B [5, 49]. For each model, we use the LongBench v2 [6] and select long-text

documents whose context lengths are around 16K, 32K, and 64K tokens. For each length, we take multiple documents and run multi-turn QA; we discard the first turn because it does not hit the prefix cache and report the average TTFT over the remaining turns that do hit the prefix cache. For the 64K case, we extend max\_position\_embeddings in the local config only to ensure the model can accept 64K tokens and we do not care about generation quality in this scenario. We report the TTFT as the main metric.

**Results.** As shown in Figure 15, across all four models and all prefix lengths, MMA consistently reduces TTFT compared to the static single-lane baseline. Depending on the model and prefix length, we observe about 1.14–2.38 $\times$  speedup over the baseline. Longer prefixes see larger improvements, because more KV cache needs to be transferred and MMA becomes more effective.

This behavior matches our motivation analysis on transfer-dominated workloads. KV cache size grows with hidden size, number of hidden layers, attention heads, and KV heads. As Qwen-7B-Chat with a 64K context, the KV cache for a single request can already reach 17.5 GB. In such cases, TTFT is largely determined by transfers rather than computation, and MMA yields a 2.38 $\times$  speedup in TTFT for large models in long-context scenarios.

### 5.2.2 Model switching with sleep mode

**Setup.** We test model switching latency under vLLM’s Sleep Mode [47]. In this mode, an idle model is evicted from GPU memory (*fall asleep*) and later reloaded (*wake up*) when requests for that model arrive again. Both phases mainly consist of moving model weights between CPU and GPU over PCIe, in *both* directions (D2H during eviction and H2D during reload).

We evaluate four Qwen models with increasing sizes: Qwen3-0.6B, Qwen3-4B, Qwen-7B-Chat, and Qwen3-32B [5, 49]. For each model, we measure the wall-clock latency of the fall-asleep and wake-up phases under the baseline and MMA.

**Results.** Figure 16 shows MMA reduces both fall asleep and wake up times substantially. For the largest model, Qwen3-32B, MMA cut fall-asleep time by about 56.8% and wake-up time by about 59.7%, roughly 2.32–2.48 $\times$  faster than the baseline. Across all four models, MMA achieves roughly 1.12–2.48 $\times$  speedup in model switching latency over the baseline.

Conceptually, end-to-end model switching time is just *old model fall-asleep + new model wake-up*, and both halves are dominated by PCIe traffic in opposite directions. MMA exploits multiple PCIe paths to speed up both H2D and D2H transfers.

In current multi-model serving systems, a single model switch often takes seconds, while front-end TTFT SLOs are typically in the sub-second range. This gap means that frequent model switching can easily hurt TTFT SLOs. Our results show that, without changing any upper-layer scheduling

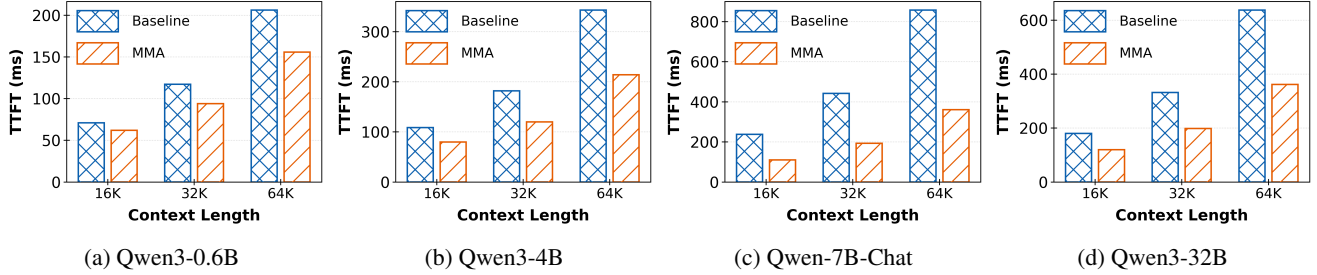


Figure 15: TTFT under different models and context length

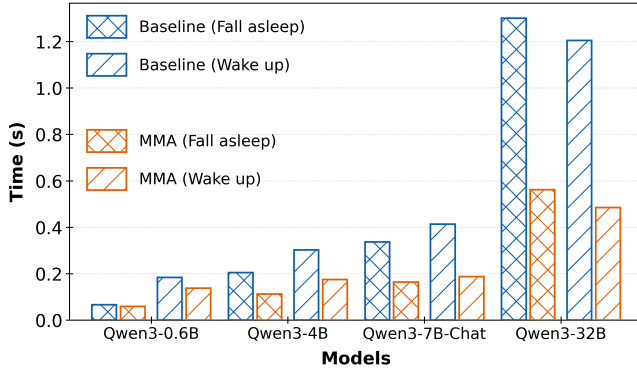


Figure 16: Fall asleep and wake up time comparison

policies, better use of PCIe bandwidth alone can cut large-model switching time by more than half, providing substantially more headroom to maintain TTFT under dynamic workloads.

## 6 Discussion and Limitations

We discuss the application scope, generality, potential and current limitations of MMA.

**MMA for intra-server data transfers.** MMA is most effective when the PCIe links between CPUs and GPUs inside a server are load-imbalanced. For example, when multiple data-parallel groups are colocated on a single server, or when prefill-decode disaggregation is combined with tensor parallelism on a server as in DistServe [52], the traffic on CPU-GPU PCIe links can become highly imbalanced across different parallel groups. In such cases, MMA can more effectively increase bandwidth and reduce end-to-end latency. However, realizing these optimizations requires additional engineering effort to integrate MMA into existing machine learning frameworks.

**Generality and potential of MMA.** The value of MMA lies in exploiting the presence of multiple heterogeneous interconnects inside a server, as well as the remaining headroom on these links; prior work has shown that, as GPU counts and the diversity of accelerators grow, this trend becomes increasingly pronounced [37, 38, 41, 43, 44]. Although MMA is only a CUDA-level software solution for accelerating GPU access to host-memory, as heterogeneous accelerators evolve,

intra-server data transfers will become an even more critical end-to-end performance bottleneck, while intra-server networks (interconnect buses) will become more diverse and expose more usable paths—and MMA takes a first step toward leveraging an asymmetric multipath fabric composed of PCIe and NVLink to accelerate intra-server GPU-host memory transfers. We hope this can serve as a starting point to motivate co-design between hardware vendors and software developers, ultimately enabling a general intra-server multipath transport layer across heterogeneous interconnects for data movement between diverse accelerators and memory devices.

**Limitations of MMA’s control plane.** In terms of implementation, the current MMA is a software-layer extension whose control plane is driven by the CPU. This software-based realization is necessary because existing hardware lacks native support for intra-server multipath scheduling. Furthermore, MMA works well for large transfers, but for fine-grained transfers the additional control and synchronization overhead can partially offset the benefits of multipath parallelism. However, our current evaluation shows that, under typical LLM workloads, the overhead of MMA’s control plane is significantly smaller than the bandwidth gains it brings, and this impact is expected to shrink further in the future. In the short term, MMA can borrow ideas from GPU-driven communication schemes such as ARK [18], offloading part of the control logic to the GPU side, and leverage the batch memory copy interface introduced in CUDA 12.8, using batched submission and weak ordering semantics to further amortize synchronization costs. In the longer term, a more desirable direction is for hardware to provide native primitives for multipath scheduling, rather than relying entirely on software “patches” to implement it.

## 7 Related Work

**CPU-GPU communication bottlenecks.** Most of prior work [8, 11, 23, 36, 46] mainly focuses on optimizing a *single* PCIe link: use multiple CUDA streams, double buffering, and asynchronous copies to overlap computation and communication. However, these approaches focus on “making one link work better” rather than “coordinating all available links.” In

contrast, MMA attempts to utilize all available CPU–GPU links and performs load balancing across these paths. To the best of our knowledge, MMA is the first system to apply multipath scheduling to CPU–GPU communication within a single server and empirically demonstrate improved effective intra-server bandwidth.

**GPU communication and inter-server multipath.** In distributed training and inference, a large body of work [13, 22, 38–40, 45] applies multipath techniques to GPU–GPU communication and inter-server bandwidth, accelerating collective operations such as AllReduce and AllToAll. FuseLink [34], for example, jointly exploits multiple NICs and intra-server GPU interconnects, using GPUs as relays to reroute traffic between NICs and improve cross-server bandwidth and NIC utilization. The key difference between MMA and FuseLink is that FuseLink builds on GPUDirect RDMA’s memory registration and metadata exchange mechanisms to implement implicit GPU relay and load-aware path selection, whereas MMA targets host-to-device data transfers within a single machine, where no RDMA or similar control channel exists. MMA therefore adopts explicit CPU–GPU relay and infers link load from local signals. The two systems are complementary at different layers and can be combined to further improve overall communication performance.

**Multipath network protocols.** At the data center network layer, MP-TCP [48] and MP-RDMA [10] have already demonstrated the effectiveness of multipath load balancing in large-scale clusters. Unlike these protocols, which operate at the inter-host network layer and can leverage congestion signals such as RTT and ECN for load balancing, intra-server CPU–GPU DMA lacks explicit feedback and can only rely on local signals. In addition, MMA brings multipath scheduling into the intra-server setting by treating PCIe, NVLink, and other CPU–GPU links as schedulable paths, providing a starting point for unified link scheduling across heterogeneous interconnects such as PCIe, NVLink, and CXL.

## 8 Conclusion

In this paper, we introduce MMA, the first multipath data transfer scheme between host-memory and GPUs. MMA employs Dummy Tasks alongside a CPU-GPU synchronization mechanism to dynamically multiplex data based on intra-server traffic within a heterogeneous CPU-GPU programming model. Through passive load balancing, MMA accurately distributes data across multiple transfer paths without requiring precise link state information. Our evaluation demonstrates that MMA effectively handles dynamic-traffic machine learning workloads, achieving high bandwidth data transfer between host-memory and GPU and accelerating ML tasks such as large language model serving and model switching.

## References

- [1] MMA code base will be opensourced after paper accepted.
- [2] Inc. Advanced Micro Devices. AMD EPYC™ 9654. <https://www.amd.com/en/products/processors/server/epyc/4th-generation-9004-and-8004-series/amd-epyc-9654.html>, 2022.
- [3] Inc. Advanced Micro Devices. AMD EPYC™ 9005 Series Processors Data Sheet. Data sheet, Advanced Micro Devices, Inc., 2024.
- [4] Reza Yazdani Aminabadi, Samyam Rajbhandari, Ammar Ahmad Awan, Cheng Li, Du Li, Elton Zheng, Olatunji Ruwase, Shaden Smith, Minjia Zhang, Jeff Rasley, et al. Deepspeed-inference: enabling efficient inference of transformer models at unprecedented scale. In *SC22: International Conference for High Performance Computing, Networking, Storage and Analysis*, pages 1–15. IEEE, 2022.
- [5] Jinze Bai, Shuai Bai, Yunfei Chu, Zeyu Cui, Kai Dang, Xiaodong Deng, Yang Fan, Wenbin Ge, Yu Han, Fei Huang, et al. Qwen technical report. *arXiv preprint arXiv:2309.16609*, 2023.
- [6] Yushi Bai, Shangqing Tu, Jiajie Zhang, Hao Peng, Xiaozhi Wang, Xin Lv, Shulin Cao, Jiazheng Xu, Lei Hou, Yuxiao Dong, Jie Tang, and Juanzi Li. Longbench v2: Towards deeper understanding and reasoning on realistic long-context multitasks. *arXiv preprint arXiv:2412.15204*, 2024.
- [7] Zhihao Bai, Zhen Zhang, Yibo Zhu, and Xin Jin. {PipeSwitch}: Fast pipelined context switching for deep learning applications. In *14th USENIX Symposium on Operating Systems Design and Implementation (OSDI 20)*, pages 499–514, 2020.
- [8] Burak Bastem, Didem Unat, Weiqun Zhang, Ann Almgren, and John Shalf. Overlapping data transfers with computation on gpu with tiles. In *2017 46th International Conference on Parallel Processing (ICPP)*, pages 171–180. IEEE, 2017.
- [9] BurnCloud. NVIDIA H20 GPU Specifications. <https://www.burncloud.com/gpu-catalog/H20.html>, 2024.
- [10] Guo Chen, Yuanwei Lu, Bojie Li, Kun Tan, Yongqiang Xiong, Peng Cheng, Jiansong Zhang, and Thomas Moscibroda. MP-RDMA: enabling RDMA with multipath transport in datacenters. *IEEE/ACM Trans. Netw.*, 27(6):2308–2323, 2019.

- [11] Yihua Cheng, Yuhan Liu, Jiayi Yao, Yuwei An, Xiaokun Chen, Shaoting Feng, Yuyang Huang, Samuel Shen, Kuntai Du, and Junchen Jiang. Lmcache: An efficient kv cache layer for enterprise-scale llm inference. *arXiv preprint arXiv:2510.09665*, 2025.
- [12] Michael Davies, Neal Crago, Karthikeyan Sankaralingam, and Christos Kozyrakis. Efficient llm inference: Bandwidth, compute, synchronization, and capacity are all you need. *arXiv preprint arXiv:2507.14397*, 2025.
- [13] Jianbo Dong, Bin Luo, Jun Zhang, Pengcheng Zhang, Fei Feng, Yikai Zhu, Ang Liu, Zian Chen, Yi Shi, Hairong Jiao, et al. Boosting large-scale parallel training efficiency with c4: A communication-driven approach. *arXiv preprint arXiv:2406.04594*, 2024.
- [14] Bin Gao, Zhuomin He, Puru Sharma, Qingxuan Kang, Djordje Jevdjic, Junbo Deng, Xingkun Yang, Zhou Yu, and Pengfei Zuo. {Cost-Efficient} large language model serving for multi-turn conversations with {CachedAttention}. In *2024 USENIX Annual Technical Conference (USENIX ATC 24)*, pages 111–126, 2024.
- [15] In Gim, Guojun Chen, Seung-seob Lee, Nikhil Sarma, Anurag Khandelwal, and Lin Zhong. Prompt cache: Modular attention reuse for low-latency inference. *Proceedings of Machine Learning and Systems*, 6:325–338, 2024.
- [16] Sylvain Gugger, Lysandre Debut, Thomas Wolf, Philipp Schmid, Zachary Mueller, Sourab Mangrulkar, Marc Sun, and Benjamin Bossan. Accelerate: Training and inference at scale made simple, efficient and adaptable. <https://github.com/huggingface/accelerate>, 2022.
- [17] John L Hennessy and David A Patterson. *Computer architecture: a quantitative approach*. Elsevier, 2011.
- [18] Changho Hwang, KyoungSoo Park, Ran Shu, Xinyuan Qu, Peng Cheng, and Yongqiang Xiong. {ARK}:{GPU-driven} code execution for distributed deep learning. In *20th USENIX Symposium on Networked Systems Design and Implementation (NSDI 23)*, pages 87–101, 2023.
- [19] Chao Jin, Zili Zhang, Xuanlin Jiang, Fangyue Liu, Shufan Liu, Xuanzhe Liu, and Xin Jin. Ragcache: Efficient knowledge caching for retrieval-augmented generation. *ACM Transactions on Computer Systems*, 2024.
- [20] Andrew G Kegel, Ronald Perez, and Wei Huang. Input/output memory management unit with protection mode for preventing memory access by i/o devices, January 14 2014. US Patent 8,631,212.
- [21] Woosuk Kwon, Zhuohan Li, Siyuan Zhuang, Ying Sheng, Lianmin Zheng, Cody Hao Yu, Joseph Gonzalez, Hao Zhang, and Ion Stoica. Efficient memory management for large language model serving with pagedattention. In *Proceedings of the 29th symposium on operating systems principles*, pages 611–626, 2023.
- [22] Ziming Li, Chenyang Hei, Fuliang Li, Tongrui Liu, Chengxi Gao, Xiuzhu Sha, and Xingwei Wang. Tuccl: Tailored and unified configuration optimizations for high-performance collective communication library. In *2025 IEEE 33rd International Conference on Network Protocols (ICNP)*, pages 1–11. IEEE, 2025.
- [23] Daniel Lustig and Margaret Martonosi. Reducing gpu offload latency via fine-grained cpu-gpu synchronization. In *2013 IEEE 19th International Symposium on High Performance Computer Architecture (HPCA)*, pages 354–365. IEEE, 2013.
- [24] Avinash Kumar Maurya, M Mustafa Rafique, Franck Cappello, and Bogdan Nicolae. Mlp-offload: Multi-level, multi-path offloading for llm pre-training to break the gpu memory wall. In *Proceedings of the International Conference for High Performance Computing, Networking, Storage and Analysis*, pages 1381–1394, 2025.
- [25] Microsoft. AzurePublicDataset: Azure LLM Inference Dataset 2023. <https://github.com/Azure/AzurePublicDataset/blob/master/AzureLLMInferenceDataset2023.md>, 2023.
- [26] John Nickolls, Ian Buck, Michael Garland, and Kevin Skadron. Scalable parallel programming with cuda: Is cuda the parallel programming model that application developers have been waiting for? *Queue*, 6(2):40–53, 2008.
- [27] NVIDIA. NVLink and NVSwitch, 2024.
- [28] NVIDIA. NVIDIA NVLink 4.0 Technology. <https://www.nvidia.com/en-us/data-center/nvlink/>, 2025.
- [29] Large Model Systems Organization. Chatbot Arena Conversations Dataset. [https://huggingface.co/datasets/lmsys/chatbot\\_arena\\_conversations](https://huggingface.co/datasets/lmsys/chatbot_arena_conversations), 2023.
- [30] Rui Pan, Zhuang Wang, Zhen Jia, Can Karakus, Luca Zancato, Tri Dao, Yida Wang, and Ravi Netravali. Marconi: Prefix caching for the era of hybrid llms. *arXiv preprint arXiv:2411.19379*, 2024.
- [31] PCI-SIG. Pci express® base specification revision 5.0 version 1.0. Technical report, PCI-SIG, 2019.

- [32] Samyam Rajbhandari, Olatunji Ruwase, Jeff Rasley, Shaden Smith, and Yuxiong He. Zero-infinity: Breaking the gpu memory wall for extreme scale deep learning. In *Proceedings of the international conference for high performance computing, networking, storage and analysis*, pages 1–14, 2021.
- [33] Zebin Ren, Krijn Doekemeijer, Tiziano De Matteis, Christian Pinto, Radu Stoica, and Animesh Trivedi. An i/o characterizing study of offloading llm models and kv caches to nvme ssd. In *Proceedings of the 5th Workshop on Challenges and Opportunities of Efficient and Performant Storage Systems*, pages 23–33, 2025.
- [34] Zhenghang Ren, Yuxuan Li, Zilong Wang, Xinyang Huang, Wenxue Li, Kaiqiang Xu, Xudong Liao, Yijun Sun, Bowen Liu, Han Tian, Junxue Zhang, Mingfei Wang, Zhizhen Zhong, Guyue Liu, Ying Zhang, and Kai Chen. Enabling efficient GPU communication over multiple NICs with fuselink. In *Proceedings of the 19th USENIX Symposium on Operating Systems Design and Implementation (OSDI 2025)*, pages 91–108. USENIX Association, 2025.
- [35] Luka Ribar, Ivan Chelombiev, Luke Hudlass-Galley, Charlie Blake, Carlo Luschi, and Douglas Orr. Sparq attention: Bandwidth-efficient llm inference. *arXiv preprint arXiv:2312.04985*, 2023.
- [36] Ying Sheng, Lianmin Zheng, Binhang Yuan, Zhuohan Li, Max Ryabinin, Beidi Chen, Percy Liang, Christopher Ré, Ion Stoica, and Ce Zhang. Flexgen: high-throughput generative inference of large language models with a single gpu. In *Proceedings of the 40th International Conference on Machine Learning, ICML’23*. JMLR.org, 2023.
- [37] Dikshant Pratap Singh, Mathialakan Thavappiragasam, and Brice Videau. Efficient intra-node hierarchical parallelisms and dynamic load balancing strategies on heterogeneous systems. In *2025 IEEE International Parallel and Distributed Processing Symposium Workshops (IPDPSW)*, pages 543–552. IEEE, 2025.
- [38] Amirhossein Sojoodi, Mohammad Akbari, Hamed Sharifian, Ali Farazdaghi, Ryan E Grant, and Ahmad Afsahi. Accelerating intra-node gpu communication: A performance model for multi-path transfers. In *Proceedings of the SC’25 Workshops of the International Conference for High Performance Computing, Networking, Storage and Analysis*, pages 449–460, 2025.
- [39] Amirhossein Sojoodi, Ali Farazdaghi, Hamed Sharifian, Ryan E Grant, and Ahmad Afsahi. Collaborative bandwidth-efficient intra-node allreduce. In *2025 IEEE International Parallel and Distributed Processing Symposium Workshops (IPDPSW)*, pages 63–67. IEEE, 2025.
- [40] Amirhossein Sojoodi, Yıltan Hassan Temuçin, and Ahmad Afsahi. Enhancing intra-node GPU-to-GPU performance in MPI+UCX through multi-path communication. In *Proceedings of the 3rd International Workshop on Extreme Heterogeneity Solutions (ExHET 2024)*. ACM, 2024. Best Paper Award.
- [41] Xiaoyong Song, Danyuan Zhou, Kai Li, Jiayuan Chen, Hao Zhang, Xiaoguang Zhang, and Xuxia Zhong. Survey of intra-node gpu interconnection in scale-up network: Challenges, status, insights, and future directions. *Future Internet*, 17(12):537, 2025.
- [42] Radostin Stoyanov, Viktória Spišáková, Adrian Reber, Wesley Armour, Marcin Copik, and Rodrigo Bruno. Engine-agnostic model hot-swapping for cost-effective llm inference. In *Proceedings of the SC’25 Workshops of the International Conference for High Performance Computing, Networking, Storage and Analysis*, pages 114–125, 2025.
- [43] Joaquin Tarraga-Moreno, Daniel Barley, Francisco J Andujar Munoz, Jesus Escudero-Sahuquillo, Holger Froning, Pedro Javier Garcia, Francisco J Quiles, and Jose Duato. Scalable and efficient intra-and inter-node interconnection networks for post-exascale supercomputers and data centers. *arXiv preprint arXiv:2511.04677*, 2025.
- [44] Joaquin Tarraga-Moreno, Jesus Escudero-Sahuquillo, Pedro Javier Garcia, and Francisco J Quiles. Understanding intra-node communication in hpc systems and datacenters. *arXiv preprint arXiv:2502.20965*, 2025.
- [45] Yıltan Hassan Temuçin, Amirhossein Sojoodi, Pedram Alizadeh, and Ahmad Afsahi. Efficient multi-path NVLink/PCIe-aware UCX-based collective communication for deep learning. In *2021 IEEE Symposium on High-Performance Interconnects (HOTI)*, pages 25–34. IEEE, 2021.
- [46] Ben Van Werkhoven, Jason Maassen, Frank J Seinstra, and Henri E Bal. Performance models for cpu-gpu data transfers. In *2014 14th IEEE/ACM International Symposium on Cluster, Cloud and Grid Computing*, pages 11–20. IEEE, 2014.
- [47] vLLM Project. Sleep Mode. [https://docs.vllm.ai/en/latest/features/sleep\\_mode/](https://docs.vllm.ai/en/latest/features/sleep_mode/).
- [48] Damon Wischik, Costin Raiciu, Adam Greenhalgh, and Mark Handley. Design, implementation and evaluation of congestion control for multipath {TCP}. In *8th USENIX Symposium on Networked Systems Design and Implementation (NSDI 11)*, 2011.

- [49] An Yang, Anfeng Li, Baosong Yang, Beichen Zhang, Binyuan Hui, Bo Zheng, Bowen Yu, Chang Gao, Chengen Huang, Chenxu Lv, et al. Qwen3 technical report. *arXiv preprint arXiv:2505.09388*, 2025.
- [50] Dongsheng Yang, Austin Li, Kai Li, and Wyatt Lloyd. Learned prefix caching for efficient llm inference. In *The Thirty-ninth Annual Conference on Neural Information Processing Systems*.
- [51] Lianmin Zheng, Liangsheng Yin, Zhiqiang Xie, Chuyue Livia Sun, Jeff Huang, Cody Hao Yu, Shiyi Cao, Christos Kozyrakis, Ion Stoica, Joseph E Gonzalez, et al. Sglang: Efficient execution of structured language model programs. *Advances in neural information processing systems*, 37:62557–62583, 2024.
- [52] Yinmin Zhong, Shengyu Liu, Junda Chen, Jianbo Hu, Yibo Zhu, Xuanzhe Liu, Xin Jin, and Hao Zhang. {DistServe}: Disaggregating prefill and decoding for goodput-optimized large language model serving. In *18th USENIX Symposium on Operating Systems Design and Implementation (OSDI 24)*, pages 193–210, 2024.